

ThermoSense: Occupancy Thermal Based Sensing for HVAC Control

Alex Beltran[†]
Elect. Eng. & Comp. Science
Univ. of California, Merced
abeltran2@ucmerced.edu

Varick L. Erickson[†]
Elect. Eng. & Comp. Science
Univ. of California, Merced
verickson@ucmerced.edu

Alberto E. Cerpa
Elect. Eng. & Comp. Science
Univ. of California, Merced
acerpa@ucmerced.edu

ABSTRACT

In order to achieve sustainability, steps must be taken to reduce energy consumption. In particular, heating, cooling, and ventilation systems, which account for 42% of the energy consumed by US buildings in 2010 [8], must be made more efficient. In this paper, we demonstrate ThermoSense, a new system for estimating occupancy. Using this system we are able to condition rooms based on usage. Rather than fully conditioning empty or partially filled spaces, we can control ventilation based on near real-time estimates of occupancy and temperature using conditioning schedules learned from occupant usage patterns. ThermoSense uses a novel multi-sensor node that utilizes a low-cost, low-power thermal sensor array along with a passive infrared sensor. By using a novel processing pipeline and sensor fusion, we show that our system is able measure occupancy with a RMSE of *only* ≈ 0.35 persons. By conditioning spaces based on occupancy, we show that we can save 25% energy annually while maintaining room temperature effectiveness.

Categories and Subject Descriptors

J.7 [Computers In Other Systems]: Command & control; C.3 [Special-Purpose and Application-Based Application Systems]: Real-time and embedded systems

General Terms

Experimentation, Measurement, Performance

Keywords

Occupancy Sensing, Thermal Sensing, HVAC Control

1. INTRODUCTION

From 1980 to 2010, energy in the United States has increased 53% [8]. In 2010, heating, ventilation, and air-conditioning

(HVAC) consumed 42% of the energy used in the United States. In order to achieve sustainability, steps to increase HVAC efficiency must take place. One method of reducing consumption is to condition based on actual usage. Rooms are often conditioned assuming constant maximum occupancy. This leads to heating or cooling empty rooms. In addition, spaces only partially occupied are over-ventilated leading to loss of conditioned air and thus thermal energy.

There are two different parts of HVAC systems usage that are affected by occupancy; temperature and ventilation. Temperature control is dependent on whether a space is occupied. In this case, a passive infrared (PIR) or ultrasonic sensor is sufficient to have a binary indication if a space is occupied. Binary sensing is common for lighting control and has also been used for temperature control [6, 15] applications. However, ventilation, used to control CO₂ levels and indoor pollutants, depends on the number of people occupying a space. One method is to simply regulate CO₂ levels directly with a CO₂ sensors. However, these systems are slow to respond and are prone to calibration errors [11]. Since standards exist for ventilating based on room occupancy [5], sensors that measure occupancy can be used to regulate ventilation. Cameras have been used for measuring occupancy [20, 9] but have several drawbacks. They are sensitive to sudden lighting and background changes. Camera placement is also an issue. Cameras placed in office spaces raise privacy concerns. While cameras can be placed in public hallways and function as an “optical” turnstile, this strategy is prone to cumulative error [9]. If an optical turnstile misses even a single person entering/exiting a space, this error is propagated until another offsetting error occurs or some other mechanism, such as assuming the room is empty at 4am, is used to remove the cumulative error. For example, if the last person in an office leaves at 6pm and this transition is missed, then the occupancy will remain erroneously at one.

In this paper, we develop ThermoSense, an occupancy monitoring system that utilizes thermal based sensing and PIR sensors. We develop a novel low-power multi-sensor node for measuring occupancy utilizing a thermal sensor array combined with a PIR sensor. The thermal sensor array used is able to measure temperatures in an 8x8 grid pattern within an 2.5mx2.5m area. We show it is possible to use these temperature readings in order to determine how many people are within the space. Unlike the CO₂ sensor, the thermal array can measure occupancy in near real-time. The thermal array is also not sensitive to optical issues, such as lighting or background changes. By adding a PIR sen-

[†]Both are primary co-authors.

Permission to make digital or hard copies of all or part of this work for personal or classroom use is granted without fee provided that copies are not made or distributed for profit or commercial advantage and that copies bear this notice and the full citation on the first page. To copy otherwise, to republish, to post on servers or to redistribute to lists, requires prior specific permission and/or a fee.

Buidsys'13, November 13-14 2013, Rome, Italy.

Copyright 2013 ACM 978-1-4503-2431-1/13/11 ...\$15.00.

sor, we increase accuracy of detecting empty spaces and the overall accuracy of the platform. The PIR sensor is also used to reduce the node’s power consumption by triggering the mote and thermal array only when someone is present. We test this new platform with a 17-node deployment covering 10 building areas totaling 2,100 sq. ft. for a period of three weeks. Using this data, we tested four different usage based conditioning strategies and analyze the energy usage; we show that 25% annual energy savings are possible with occupant based conditioning strategies. In this paper, we contribute the following:

- We developed a novel multi-sensor platform for estimating occupancy utilizing a thermal sensor array and a PIR sensor. We performed a full system power consumption analysis and tested a 17-node deployment over a 3 weeks, in 10 HVAC conditioning areas, covering 2,100 sq.ft.
- We developed a new occupancy classification process using the sensor data, which includes thermal map background update, feature extraction, occupancy classifiers and post-processing filtering. We tested three classifiers, including K-Nearest Neighbors (KNN), Artificial Neural Networks (ANN), and linear regression (LR). Using this process, we showed that these types of sensors are capable of estimating occupancy with an RMSE of *only* ≈ 0.35 persons.
- We tested four different strategies for HVAC conditioning and show how different sensing and actuation strategies affect energy consumption and occupant comfort. We showed that by using this system for conditioning usage based control of temperature and ventilation we can save 25% energy annually while maintaining occupant comfort.

2. RELATED WORK

The authors of [13] test the use of cameras as optical turnstiles to estimate occupancy. However, they fail to address how cumulative error can impact occupancy estimates. As previously mentioned, even a single error will cause error to propagate forward. The total ground truth was also limited to 4 hours total for different times of the day.

The authors of [9] also use cameras as optical turnstiles. They mount multiple strategically placed cameras in hallways to measure occupancy for several areas. In addition, they also have a PIR sensor network in order to better distinguish empty rooms. Again, the major drawback to this approach is the cumulative error that will occur. However, unlike [13], they discuss strategies for reducing cumulative error. They impose maximum occupancy limits and use a particle filter with an occupancy model with live data to estimate the error. However, since their approach uses a model, their approach also requires a non-trivial amount of ground truth occupancy data (2 weeks), collected using webcams. The occupancy RMSE achieved was 1.83 persons, more than 5 times the ThermoSense’s error.

In [7], elderly people are tracked using Imote2 motes with Enalab cameras and utilizing a motion histogram for a period of 1 week. Occupant counts are achieved by counting peaks within the histograms. Their system also includes PIR sensors in order to detect occupancy for certain areas. There are several drawbacks to this approach. Since the camera must continually poll the room in order to generate the motion histograms, the power consumption during periods of occupancy will be high. The problem of privacy also exists for this system; cameras must be placed directly in the room.

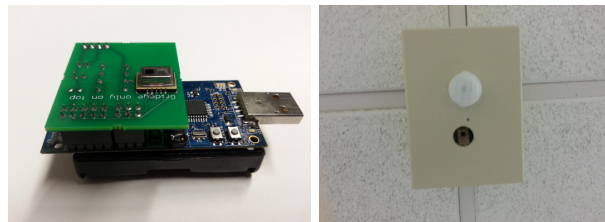


Figure 1: Grid-Eye attached to a Tmote (left). Enclosure containing both the Grid-Eye and PIR (right).

The papers [15, 6] describe methods that uses door sensors with PIR sensors to obtain a binary measurement of occupancy. Ground truth data was collected using surveys and manual annotations, and the experiments were run for 1-4 weeks and 4 days respectively. By adding door sensors, they minimize instances where overly still occupants become invisible to the PIR sensor. While this technique improves the binary measurement of occupancy, these systems do not provide a precise occupancy estimate.

Rather than rely on PIR sensors alone, the authors of [18] also utilize active radio frequency identification (RFID) tags to determine occupancy. By deploying multiple antennas with the occupied space, the RFID tags were able to broadcast their presence every 5 seconds. The limitation to this strategy is that every occupant must possess a RFID tag, and that tag must always be co-located with the occupant.

The papers [14, 16] estimates occupancy by measuring a variety of parameters. They collected ground truth data for 5 and 1 weeks deployments, using video camera and a user voluntary electronic tally counter to measure room occupancy respectively. In these deployments, they utilize multiple sensors to estimate occupancy; CO₂, CO, lighting, temperature, humidity, motion, and acoustics. For each parameter, they define multiple feature vectors, which are then used with several models to estimate occupancy. While this multi-sensor approach works well for the sole purpose of occupancy estimates, this approach will not work well if combined with a ventilation strategy. They assume that ventilation will not affect occupancy estimates of the room. However, since ventilation will affect CO₂ and humidity levels and thus occupancy estimates, it is likely that ventilation rates based on occupancy estimates from this system will lead to wild fluctuations in ventilation actuation and periods of under-ventilation. In this case, ventilation is better controlled by CO₂ sensors directly even with the known calibration and response time issues [11]. In essence, if CO₂ or humidity is used as sensory input, you can either control ventilation or estimate occupancy, not do both at once.

3. THERMOSENSE

In this section we discuss ThermoSense, a wireless sensor network of nodes that can measure occupancy using a combination of thermal readings and PIR. Figure 1 shows the ThermoSense node used for the sensor network.

In order to have an effective wireless occupant measurement system suitable for HVAC control, several design considerations must be examined. While wired system for binary occupancy sensing exists, these systems are costly to install and can be difficult to retrofit into older buildings; for our system, we want an easy to deploy wireless system. Since it is wireless, power consumption is a significant is-

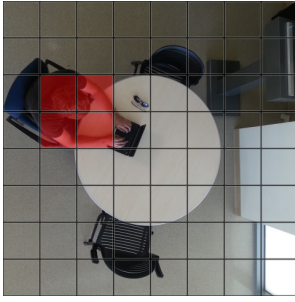


Figure 2: 8x8 thermal array sensing an occupant.

Components Used	Energy Usage.
Mote Only	4.72 mA
Mote + PIR	4.73 mA
Mote + PIR + Grid-Eye	4.76 mA
Mote + PIR + Grid-Eye + Radio	4.82 mA

Table 1: Energy Usage for independent components.

sue. Both the mote and sensors must be low-powered and run in a power efficient manner. For our platform, we make use of a PIR for two reasons. The first is that accurate detection of empty rooms is critical in order to capitalize on potential savings. The second is that the PIR can also be used to sleep components in the system when sensing and communication are not necessary. While the PIR is able to give an accurate and reliable binary indication of occupancy, we need another sensor capable of determining how many occupants are in an area. Since occupants are typically warmer than the surroundings, a thermal sensor array, capable of measuring multiple temperatures with an area, is viable method for detecting occupancy. Figure 2 shows an above view of the area, where each square of the grid is a point of measurement of the thermal sensor array. The shaded red squares shows the points in the grid with higher temperatures, which in this case is the location of the occupant. Multiple occupants can be distinguished by higher density of warmer temperatures.

3.1 Hardware

Each ThermoSense node contains a Tmote Sky, PIR, and Grid-Eye Sensor. The Tmote Sky [19], produced by MoteIV, has a 8MHz TI-MSP430 micro-controller with 48k Flash storage and 10k RAM. The Tmote communicates using a Chipcon CC2420 radio. The PIR sensor is connected to the Tmote’s digital input/output pin while the Grid-Eye is connected to the I2C clock and data pins. We developed a board in order to connect both the Grid-Eye and PIR sensor with the Tmote.

The PIR used in the nodes is the PaPIR EKMB VZ series developed by Panasonic. The PIR is able to detect motion up to 12m with a detection a viewing angle of 102°x92° horizontal by vertically respectively [3]. The infrared thermal array used to detect actual occupancy is the Grid-Eye sensor made by Panasonic [2], priced at \$31. This sensor measures 64 temperatures in an 8x8 grid where the physical size of this grid is determined by the distance the sensor is to the target surface. We found the Grid-Eye to be able to sense within a 2.5mx2.5m square when placed at a height of 3m. The Grid-Eye measures temperatures from -20C° to 80C° with an accuracy of $\pm 2.5C^\circ$ and can sample 10 times per second (each sample contains 64 temperature values).

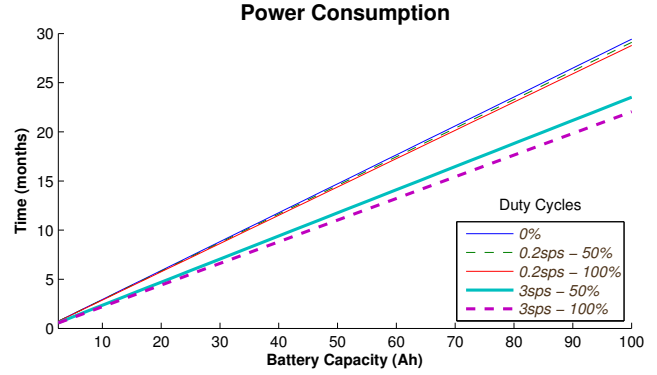


Figure 3: Energy usage for different duty cycles.

3.2 Power Consumption

We used two 3000 mAh lithium batteries for each node in our deployment. We found battery life of ThermoSense node to be over three weeks sampling once every five seconds. For a more detail analysis of the consumption, we measure each component of the platform separately using an oscilloscope. Table 1 summarizes the results. The difference in energy between using PIR and Grid-Eye together as compared to the PIR only is small (0.03 mA). Adding the radio with the Grid-Eye and PIR only increases the current use by 0.06 mA. Since the samples were only sent once every 5 seconds, the energy use of the radio is small. Figure 3 shows the lifetime of the system at different duty cycles for different battery capacities. Since we have access to 80 Ah batteries that fit in our enclosure, we can estimate how long this system would last with larger capacity batteries. We can see even in the worse case, an 80 Ah battery would last longer than 1 year. If we were to sleep various components of the mote and if we were to do smart local data processing to transmit only deviations from a model, we could even further reduce power consumption and extend system lifetime. These optimizations are left for future work.

4. OCCUPANCY CLASSIFICATION

In this section, we develop the process for occupancy classification in order to estimate occupancy from the ThermoSense node. Figure 4 shows an overview of this process. Information from the PIR and thermal sensors is used to update and maintain background levels of the thermal map. The current values along with the current background are used to create features vectors. These feature vectors are inputted into a classification model, which produces a “raw” occupancy estimate. A filter is then applied to the “raw” occupancy along with past occupancy estimates to produce the final occupancy estimate.

In the following sections, we develop and analyze each component of the occupancy classification process and examine the overall performance of the resulting occupancy estimates. We first examine the performance of the PIR sensor, and examine in particular the ability of the sensor to detect empty rooms. We next describe the process used to maintain the thermal background using the thermal array and PIR sensor. Then we describe how the background and current thermal map is used to create the feature vectors used for the occupancy classification model. We examine three different classification models; K-nearest-neighbors

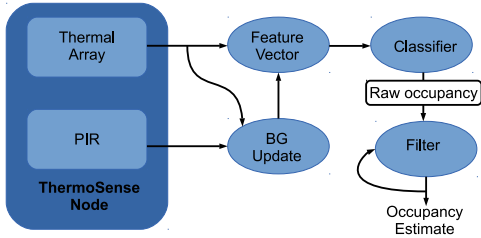


Figure 4: Occupancy Classification Process

(KNN), linear regression (LR), and artificial neural networks (ANN). We then discuss the use of the filter on the “raw” occupancy output of the models. Finally, we examine how the final output of the process performs by comparing the output to ground truth data collected over a 24-hour period of time from manually processed video feeds.

4.1 PIR Sensor Input

In our ThermoSense nodes, the PIR is used to detect if a room is currently occupied or unoccupied. The nature of the PIRs only allows motion detection, but people are not constantly moving when they are occupying a room. The PIR signal constantly fluctuates when motion is detected, and this requires a smoothing method to process it. Therefore, we smooth the raw PIR values over a period of 8 minutes. This period was found by evaluating multiple different time windows and it is sufficient time to allow someone to remain inactive for a short time while still being able to detect that the room is being used. An 8 minute period was also found to return the least number of false positives. These false positives can occur when a person momentarily enters a room (e.g. a janitor) or positives that continue to be returned after a person has left a room (e.g. motion activity before leaving). This smoothing compared to ground truth can be seen in Figure 5.

Due to low number of false negatives, seen in Figure 6, the PIR can be used reliably as an unoccupied indicator. This can be used to override any predictions that would normally be made by our thermal array sensor. Once a room has been established as occupied by the PIR, additional models can be used to further evaluate the actual occupancy of a room.

4.2 Thermal Background

Since occupants are typically by far the warmest objects in a conditioned room, the thermal array can be used to detect occupants within a space. However, in order to distinguish between passive warm objects such as computers or refrigerators and humans, we maintain a thermal background map. If the PIR sensor indicates the room is empty, then this information can be used to determine the thermal background of the space. As the background can change over time, this background is continuously updated. In addition to maintaining the background, the standard deviation of each grid position is also saved; this standard deviation is used in the following section as a thresholding parameter for distinguishing significantly warm grid components. Algorithm 1 defines how our current background and standard deviation for each pixel for this background is maintained. a If the PIR has detected no movement for the 15 previous minutes, the background is updated using an exponential weighted moving average (EWMA) and the standard deviation is updated for each grid component. We found 15

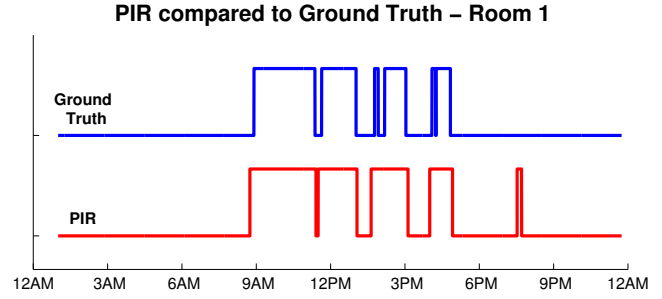


Figure 5: PIR compared to ground truth.

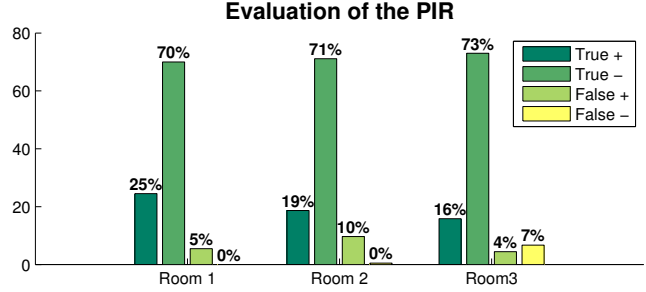


Figure 6: PIR evaluation of all three rooms

minutes worked best, as it is unlikely an occupant remains motionless for 15 minutes. This threshold is also commonly used for PIR based lighting control [4]. However, if an occupant occupies a space for a significant period, it is possible that the background changes during this period. To adjust the background while the space is occupied, we chose a few grid points with the lowest temperatures as our scaling components. The points with the lowest temperatures are most likely unoccupied and can be used to update the old background. We divide these scale points with the old background and average them to find a multiplier we can use to update our previous background. We then multiply the scale to the old background to find out a new background. The new background is smoothed into our old background by using an EWMA but with a significantly lower weight applied.

4.3 Feature Vectors

We next define feature vectors that we will use as input for the classification models. While it is possible utilize all 64 values of the thermal array along with the PIR sensor, we found that this approach did not generalize well; the models would not work well when applied to different areas. Instead, we use the following three features for our models; the total number of significantly warm points, the number of grouped points that are warm, and the size of the largest group of warm points. The following subsections formally defines how we extract these features. We tried a significant number of other less successful feature vectors, e.g. 64 raw values, 64 thresholded-binary values, size of all connected components, different permutations of the feature vectors, etc., but cannot discuss these due to space limitations.

All three feature vectors are based on identifying the significantly warm points on the grid. As our first step, we first create a 8x8 binary matrix representing the significantly warm points from the thermal map. This is done by taking

Algorithm 1 Background Update

```

EWMA( $a, x, y$ )  $\leftarrow$  EWMA with weight  $a$ .
minTemp( $f, n$ )  $\leftarrow$  indices of the  $n$ -lowest temperatures from
frame,  $f$ 
frame  $\leftarrow$  current frame
newBg  $\leftarrow$  returned updated background
oldBg  $\leftarrow$  old background
windowBG  $\leftarrow$  sliding window of the background

if PIR has been off for more than 15 minutes then
  newBg = EWMA(0.1, oldBg, frame)
  add frame to windowBG
  threshold  $\leftarrow$  3 * std(windowBG)
else
  indeces  $\leftarrow$  minTemp(frame, 5)
  for each index in indeces do
    scalePx(index)  $\leftarrow$  oldBg(index)/frame(index)
  end for
  scale  $\leftarrow$  mean(scalePx)
  scaledBg  $\leftarrow$  scale * frame
  newBg = EWMA(0.01, oldBg, scaledBg)
end if

```

the difference between the background and the current thermal map and applying a standard deviation based threshold to this difference. We define current thermal values, background, and standard deviation as $M_{ij} = (m_{0,0}...m_{7,7})$, $B_{ij} = (b_{0,0}...b_{7,7})$, $S_{ij} = (s_{0,0}...s_{7,7})$, respectively. An active point is defined as being three standard deviations away from the background,

$$f(i, j) = \begin{cases} \text{True,} & \text{if } M_{i,j} - B_{i,j} > 3 * S_{i,j} \\ \text{False,} & \text{if } M_{i,j} - B_{i,j} < 3 * S_{i,j} \end{cases}$$

Feature 1: Total Active Points - For our first feature, we use the total number of active points. A larger total is correlated with higher number of occupants.

Feature 2: Number of Connected Components - Our second feature is based on connected components [12]. Connected components is a method of identifying groups of points within a matrix that are connected to each other. A point is considered connected if it is the same value as the point diagonal or directly adjacent. A component is a group of connected points. The number of the components, which are number of grouped warm points in our application, is correlated to the number of people occupying the area.

Feature 3: Size of Largest Component - The third feature is the size of the largest component with the grid. Multiple occupants standing close together will create one large component rather than several separate components which would results in a lower occupancy count. The size of the largest component is positively correlated with occupancy and can be used to get a more accurate count.

4.4 K-Nearest Neighbors

The first model we consider is K-Nearest Neighbors. Let $X = (x_0...x_n)$ be the the components of the feature vector of the current frame. $Y = (y_0...y_n)$ is each individual feature components found inside the entire training set, $Z = (Y_0...Y_m)$. We use euclidean distance to calculate the distance between feature vectors,

$$d(X, Z_j) = \sqrt{\sum_{i=0}^n (x_i - Z_{ji})^2}$$

We then find the minimum k distances from the training set of Z and collect the distances as $D = (d_0...d_k)$ with it's

	Value	p-value
β_A	0.141	2.44×10^{-187}
β_S	-0.051	1.14×10^{-30}
β	0.201	9.25×10^{-11}
F-statistic	3220	≈ 0
R^2	0.858	

Table 2: Parameters of linear model and fit metrics.

corresponding occupancy labels as $L = (l_0...l_k)$. Weight is applied depending on the distance to each labels to get the final predicted occupancy, P .

$$P = \sum_{i=0}^k w_i l_i, \text{ where } w_i = 1 - d_i / (\sum_{j=0}^k d_j)$$

When calculating KNN, we find the 5 nearest neighbors and the distances associated with each. The predicted occupancy is averaged with the labels associated with the 5 closest values, with the largest weight given to values with the smallest distance.

4.5 Linear Regression

The next model we examine is a linear regression model. We define a linear model

$$y = \beta_A A + \beta_S S + \beta$$

where y is the estimated occupancy (predicted variable), A is the number of active pixels and S is the size of the largest component (indicator variables). β_i is the corresponding coefficient for the indicator variable i and β is a constant. While the other models also included the number of components as a parameter, for the linear model, we chose A and S by testing permutations of the feature vectors that minimized root mean squared error (RMSE) and had significant coefficients ($p < 0.05$). We also found that the model fit best when estimating positive occupancy. Thus, we train the linear model with data for the 1, 2, and 3 person cases and rely on the PIR sensor to determine if a space is empty.

Table 2 shows the fitted model parameters along with p values of each parameter and the F-test of the overall model. Using a $p < 0.05$ threshold, we see the p -values for each of the indicator variables is significant. We see also find that $p \approx 0$ from the F-test and $R^2 = 0.858$, indicating a good fit. Figure 7, shows the distribution of the residuals. The normal distribution verifies that the independent error assumption has not been violated.

4.6 Artificial Neural Network

The final model we consider is a forward feed ANN [17] using a single hidden layer of 5 perceptrons. We use a sigmoid for the hidden layer transfer function and a linear transfer function for the output layer. The same data for the 1, 2, and 3 person case was used for the ANN model. Again we use the PIR value to determine the 0 person case. We used 70% of the data for training, 15% for testing, and 15% for validation. We found $R^2 = 0.893$ and $R^2 = 0.906$ when compared with the testing set and the entire dataset respectively, suggesting the model has a strong fit.

4.7 Filter

The last step of the occupancy classification process is the filtering of the raw occupancy estimate. If we examined the error of the models, we found that the errors are independent and normally distributed (see Figure 7). Thus, we employ a 4 minute moving average filter in order to reduce error

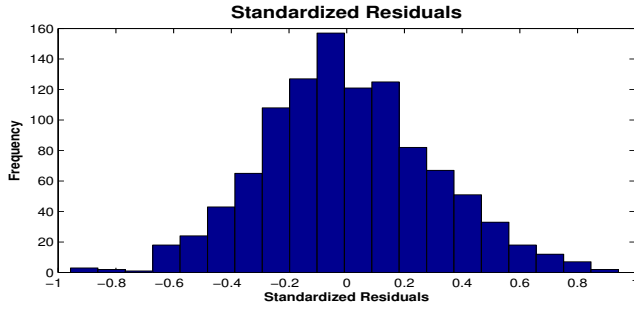


Figure 7: Plot of residual distribution

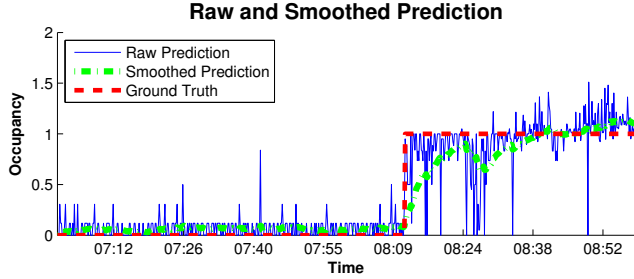


Figure 8: Model raw and filtered outputs.

of the raw occupancy estimate produced by the classification model. We found that the 4 minute window minimized our error and was found through trial and error. Figure 8 compares the raw output of the model with the filtered output. From the figure, we can see that the filter is effective at removing independent errors.

4.8 ThermoSense Performance

In this section, we examine the performance of the process with respect to the three models. In order to test the performance, we gathered 24 hours of ground truth data. This data was gathered by deploying a camera in a public hall way and manually counting the number of people entering and leaving the zone through out the day. For our analysis, we examined a single zone comprised of 3 separate offices. For our performance metrics, we use RMSE and normalized root mean squared error (NRMSE).

Table 3 summarizes the performance results. Overall KNN, performed the best. KNN had a RMSE of 0.346 people (NRMSE of 11.5%). LR and ANN had slightly higher RMSE values of 0.409 people and 0.385 people (NRMSE of 13.6% and 12.8%) respectively. Figure 9 shows the performance of the models as a function of the amount of training data available. In particular, KNN is able to perform fairly well relative to the amount of data available. With only 100 training samples, KNN has a NRMSE value of 25%. Both LR and ANN have values 35% and 34% respectively when trained with the same 100 samples. LR and ANN have very similar performance between 100-900 samples. After 900 samples, we see that the ANN starts to have slightly better performance than LR. Though KNN maintained lower NRMSE overall, the difference among the different models became small as the available data increased; the maximum difference among models is only 2.1%.

4.9 Model Discussion

While each model had similar results with KNN having the

	KNN	LR	ANN
RMSE	0.346	0.409	0.385
NRMSE	11.5%	13.6%	12.8%

Table 3: Evaluation of the models used.

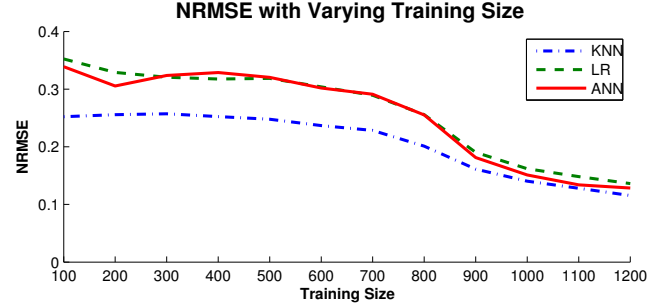


Figure 9: NRMSE of a ThermoSense node in a zone.

best RMSE, there are other issues to be considered. KNN required the least amount of data in order to achieve a low NRMSE. However, Figure 9 shows that as more training data is available, the other models may well match or outperform KNN. Another consideration is that as the number of training data increases, the run-time performance of KNN will decrease. While there is a possibility of running KNN on a mote, it requires storing the entire training set and iterating through the set for each new sensed sample. Thus, KNN is more suited to situations with little data exists and KNN is processed at the base-station rather than the node. Though the linear model had the lowest accuracy, there are other advantages to this approach. In particular, it can be run very efficiently on a mote; in our case, only the values of the coefficients (β, β_A, β_S) need to be stored on the mote and new estimates are simple to calculate in real-time. A similar argument can be made for ANN; only the input and weights need to be stored on the mote and estimates are trivial to calculate in real-time. ANN can require potentially more time to train, but as this is a one time cost, ANN may be preferable over LR since ANN can handle non-linearities.

5. ENERGY ANALYSIS

With the occupancy estimation system in place, we next would like to use data collected from the ThermoSense system to estimate potential energy saves using different strategies. Since KNN had the best performance in terms of RMSE and NRMSE, we use this model for our energy analysis. In this section, we evaluate four strategies to reduce energy usage and compare them to a baseline strategy that operates on a static schedule. We use the OBSERVE strategy described in [10]. The OBSERVE method utilizes a Blended Markov Chain (BMC) that continuously updates its prediction based on the current occupancy estimate. If trained with binary data, this model can give binary predictions of occupancy. With discrete training data, the model is able to predict discrete levels of occupancy. Based on a probability threshold, the room is conditioned beforehand if the room is likely to be occupied in the coming hour. Ventilation is controlled according to ASHRAE 62.1 [5]. For our analysis we use predictions discrete occupancy, binary predictions, and a purely reactive strategy using no prediction.

We trained the BMC's using 3 weeks of data collected from the ThermoSense system deployed in 8 offices, 1 lab and 1

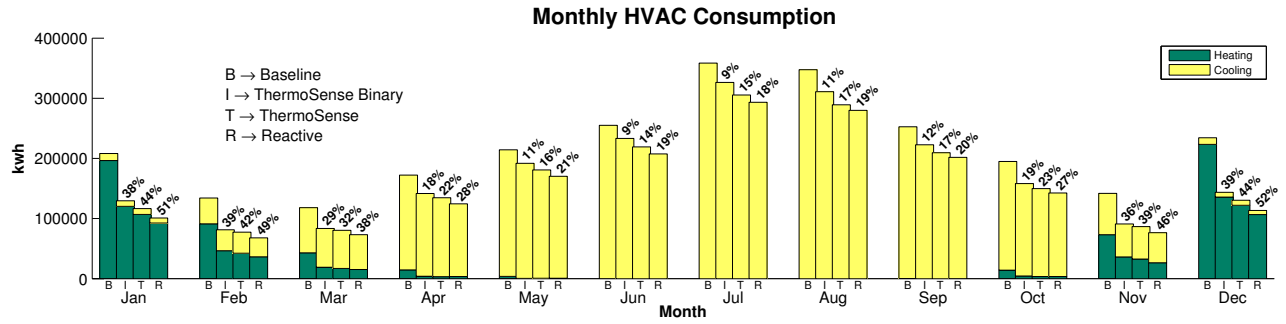


Figure 10: Monthly heating and cooling consumption for the different strategies.

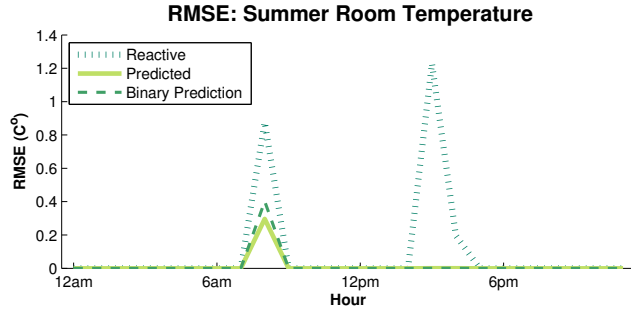


Figure 11: The temperature RMSE for the periods when the room was occupied during the summer.

conference room in an academic commercial building. Using the BMC, we generated 7 days of simulated occupancy. To simulate system error, we introduced error based on a normal error distribution. This distribution was determined by examining the distribution of the residuals from our RMSE analysis and performing a normal fit. The frequency of these perturbations was added using an exponential distribution. We found that the duration between the errors were exponentially distributed.

To test these strategies, we utilize EnergyPlus [1], which is a state-of-the-art industry standard tool for simulating buildings. With this simulator, we are able to change occupancy over time to determine how these strategies affect efficiency. By using a simulator, we are also able to test the strategies under identical weather conditions. In our simulation, we used materials similar to the actual building and sized rooms to match the deployment. Target set-points of 24C° (75.2F°) and 20C° (68F°) was used for cooling and a heating set-points respectively. Since our deployment only covered part of the entire building, we assumed the same schedules for the rest of the building in the simulation. The simulated commercial building contains offices, labs, and meeting rooms. The location of the simulation was in the central valley of California. Other locations were not evaluated in the interest of space.

Figure 10 shows the monthly breakdown of the heating and cooling. All three strategies had significant energy savings over the baseline strategy. Overall, the reactive strategy had the lowest energy consumption. This strategy consumed 29.6% less than the baseline strategy annually. It saves additional energy since it does not pre-condition rooms ahead of time. However, we will see that this savings in energy comes at the cost of comfort (Section 6). In general, all

the strategies had the largest percentage of savings during winter months (Nov - Feb) and the lowest percentage of savings during the warmer months (May - Sep). ThermoSense and ThermoSense Binary had 24.8% and 19.7% savings respectively. The binary approach consumed more energy since this strategy has a tendency to over-ventilate. Over-ventilation reduces efficiency since it increases the amount of outside air that needs to be conditioned. The greatest differences between the ThermoSense and ThermoSense Binary approaches occur during the warmest and coldest months (Jan, Dec, Jul, Aug) where ThermoSense consumed 5-6% less than ThermoSense Binary. Increased ventilation of ThermoSense binary during these months has a greater impact on efficiency than during milder shoulder seasons.

6. CONDITIONING EFFECTIVENESS

In the previous section, we show that occupant based conditioning saves a significant amount of energy. However, conditioning effectiveness also needs to be considered.

For the temperature effectiveness, we examine a room that is only occupied at 8am, 3pm, and 4pm on Mondays and focus our analysis to the warm months (May - Sep). For our analysis, we examine the RMSE of the room temperature from the target temperature for each hour. Figure 11 shows the RMSE for each hour of the day. For un-occupied periods, we consider the RMSE to be 0. The reactive strategy had the worst overall performance. At 8am, the RMSE was 0.877C° during the hour that the room was occupied. At 3pm the room had a RMSE of 1.23C°. This higher RMSE is due to the solar gain increasing the temperature of the room. However, at 4pm the RMSE drops to 0.197C°. In this case, the occupied state of the room at 3pm carried over to the 4pm period. Thus, while some energy was saved by not pre-conditioning, we can see that this was at the cost of thermal conditioning. Both ThermoSense prediction strategies perform substantially better than the reactive strategy. At 8am the ThermoSense and ThermoSense Binary prediction methods had RMSE values of 0.309C° and 0.415C° respectively. At 3pm-4pm, both prediction strategies had nearly identical RMSE values; both were close to 0.033C°. Again, while the ThermoSense prediction strategies consumed slightly more energy, they did not compromise thermal conditioning.

Next we examine the ventilation effectiveness of the system. For our analysis, we evaluate the ventilation of the spaces for one particular day. As previously mentioned, we use the ASHRAE 62.1 standard to determine the ventilation according to occupancy. As ventilation is regulated in real-time, the binary based strategies (reactive and Ther-

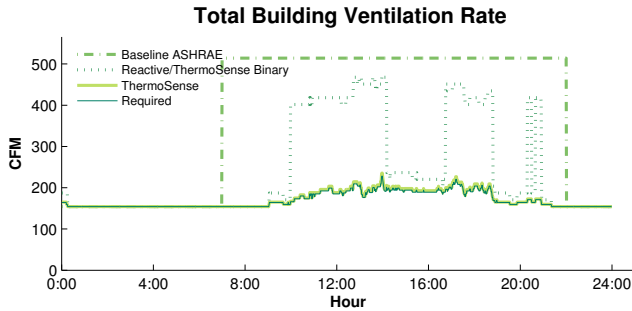


Figure 12: Ventilation effectiveness of the strategies.

moSense binary prediction) have the same ventilation rates. As we cannot determine the precise occupancy with a binary occupancy estimate, we assume maximum occupancy for rooms that are occupied for ventilation. The baseline strategy assumes maximum occupancy from 7am to 10pm. Figure 12 shows the baseline, ThermoSense binary, and ThermoSense based strategies. We can see that the baseline strategy greatly over-ventilates. However, there is also a short period at the beginning where the baseline strategy under-ventilates; this illustrates the shortcomings of a static schedule. Both the ThermoSense binary and ThermoSense strategies were able to meet the required ventilation level. However, we can see that the ThermoSense binary strategy still over-ventilates the area a great deal; overall, this strategy over-ventilated the area by 170%. The ThermoSense binary strategy performed best when multiple rooms were empty, which can be seen during the period between 2pm and 5pm. Since only a few rooms were occupied, only a few rooms were over-ventilated. The ThermoSense based ventilation performed the best. We can see that the ventilation rate is only 3.25% more than the required rate. This is due mainly to a 10% occupancy increase added by design in order to protect against under-ventilation that could be caused by sensor errors [10].

7. CONCLUSIONS

In this paper, we developed ThermoSense, an occupancy monitoring system that utilizes thermal based sensing and PIR sensors. We developed a novel low-power multi-sensor node for measuring occupancy using a thermal sensor array combined with a PIR sensor. The thermal sensor array is able to measure temperatures in an 8x8 grid pattern within an 2.5mx2.5m area. We showed it is possible to use these temperature readings in order to determine how many people are within the space using a novel occupancy classification process. Unlike the CO₂ sensor, the thermal array can measure occupancy in near real-time. The thermal array is also not sensitive to optical issues, such as lighting or background changes. By adding a PIR sensor, we increased accuracy of detecting empty spaces and the overall accuracy of the platform. The PIR sensor is also used to reduce the node's power consumption by triggering the mote and thermal array only when someone is present. We tested this new platform with a 17-node deployment covering 10 building conditioning areas totaling 2,100 sq. ft. for a period of three weeks and showed that ThermoSense is able to detect occupancy with a RMSE of *only* ≈ 0.35 persons. Using this data, we tested four different usage based conditioning strategies and analyzed the energy usage; we showed

that 25% annual energy savings are possible with occupant based conditioning strategies.

8. ACKNOWLEDGMENTS

We would like to thank the reviewers for their constructive comments. We also like to thank Daniel Winkler for his help with the deployment and energy measurements, and John Lusby for the development of the sensor boards. This material is based upon work partially supported by the National Science Foundation under grant #CNS-1254192, and CITRIS under grant #CITRIS-SPF-165.

9. REFERENCES

- [1] Energyplus. <http://apps1.eere.energy.gov/buildings/energyplus/>.
- [2] Grid-eye. <http://pewa.panasonic.com/downloads/grid-eye/>.
- [3] Panasonic PIR. <http://pewa.panasonic.com/downloads/papirs-ekmb/>.
- [4] Occupancy sensors, motion-sensing devices for lighting control. *Lighting Research Center*, 1998.
- [5] ASHRAE standard 62.1: Ventilation for acceptable indoor air quality. ASHRAE, Inc., 2007.
- [6] Y. Agarwal, B. Balaji, S. Dutta, R. K. Gupta, and T. Weng. Duty-cycling buildings aggressively: The next frontier in HVAC control. In *IPSN'11*.
- [7] A. Bamis, D. Lymberopoulos, T. Teixeira, and A. Savvides. The behaviorscope framework for enabling ambient assisted living. *Personal Ubiquitous Computing*, 14(6):473–487, Sept. 2010.
- [8] DOE. *2010 Building Energy Data Book*. U.S. Dept. of Energy, 2011.
- [9] V. Erickson, S. Achleitner, and A. E. Cerpa. POEM: Power-efficient occupancy-based energy management system. In *IPSN'13*.
- [10] V. L. Erickson, M. Á. Carreira-Perpiñán, and A. E. Cerpa. OBSERVE: Occupancy-based system for efficient reduction of HVAC energy. In *IPSN'11*.
- [11] W. J. Fisk. Accuracy of CO₂ sensors in commercial buildings: a pilot study. Technical Report LBNL-61862, 2006.
- [12] J. Hopcroft and R. Tarjan. Algorithm 447: efficient algorithms for graph manipulation. *Commun. ACM*, 16(6):372–378, June 1973.
- [13] A. Kamthe, L. Jiang, M. Dudys, and A. Cerpa. SCOPES: Smart cameras object position estimation system. In *EWSN'09*.
- [14] K. P. Lam, M. Hoynck, B. Dong, B. Andrews, Y.-S. Chiou, R. Chang, D. Benitez, and J. Choi. Occupancy detection through an extensive environmental sensor network in an open-plan office building. In *International Building Performance Simulation Association*, 2009.
- [15] J. Lu, T. Sookoor, V. Srinivasan, G. Gao, B. Holben, J. Stankovic, E. Field, and K. Whitehouse. The smart thermostat: using occupancy sensors to save energy in homes. In *SenSys'10*.
- [16] S. Mamidi, R. Maheswaran, and Y. Chang. Smart sensing, estimation, and prediction for efficient building energy management. In *Multi-agent Smart Computing Workshop*, 2011.
- [17] T. M. Mitchell. *Machine Learning*. McGraw-Hill, New York, 1997.
- [18] J. Scott, A. J. B. Brush, J. Krumm, B. Meyers, M. Hazas, S. Hodges, and N. Villar. Preheat: controlling home heating using occupancy prediction. In *UbiComp'11*.
- [19] T. Sky. <http://www.snm.ethz.ch/Projects/TmoteSky>.
- [20] T. Teixeira and A. Savvides. Lightweight people counting and localization in indoor spaces using camera sensor nodes. In *ICDSC'07*.